https://doi.org/10.15407/scine21.02.073

RUSANOV, R. A. (https://orcid.org/0000-0003-2930-2574),
RUSANOV, A. V. (https://orcid.org/0000-0002-9957-8974),
and CHUGAY, M. O. (https://orcid.org/0000-0002-0696-4527)

A. Pidhornyi Institute of Power Machines
and Systems National Academy of Sciences of Ukraine,
2/10, Komunalnykiv St., Kharkiv, 61046, Ukraine,
+380 57 293 0144, ipmach@ipmach.kharkov.ua

ANALYSIS OF THE INFLUENCE OF OPERATIONAL AND GEOMETRICAL CHARACTERISTICS ON THE EFFICIENCY OF AXIAL TURBINE STAGE PROFILE CASCADES

Introduction. *Bladed rotary machines have been extensively utilized across various industries for over a century, particularly in axial turbines and turboexpanders, including steam and gas power turbines as well as aircraft gas turbine engines.*

Problem Statement. *Advances in modern design methodologies and manufacturing technologies have enabled the development of axial turbines with significantly high gas-dynamic efficiency. This efficiency is primarily determined by irreversible kinetic energy losses in real flow processes compared to ideal, isentropic processes. In contemporary turbine designs, kinetic energy losses under nominal operating conditions have frequently been reduced to below 10%. However, it remains critical to establish the absolute minimum kinetic energy losses achievable in axial turbines under specific operating conditions.*

Purpose. *This study investigates the effects of operational and geometric parameters — including the effective stator angle, Reynolds number, and dimensionless conditional rate of thermal drop — on the efficiency of profile cascades in axial turbine stages of both active and reactive types.*

Materials and Methods. *State-of-the-art numerical modeling techniques for turbomachinery flow path design and calculation, implemented through the IPMFlow software package, have been employed in this study.*

Results. *The research has identified new correlations and mechanisms for enhancing the gas-dynamic efficiency of axial turbine profile cascades. For each examined operating condition and geometric configuration, profile cascades have been designed based on the principle of "rational" aerodynamic optimization, yielding efficiency values close to their theoretical maximum. Findings indicate that for Reynolds numbers exceeding 5×10^6, kinetic energy losses in profile cascades can be reduced to below 2%.*

Conclusions. *The study has provided new insights and design principles that can be applied to the development and modernization of axial turbines, contributing to further improvements in their overall efficiency.*

Keywords: design methods, gas-dynamic efficiency, turbine flow part, active type stage, reactive type stage.

Citation: Rusanov, R. A., Rusanov, A. V., and Chugay, M. O. (2025). Analysis of the Influence of Operational and Geometrical Characteristics on the Efficiency of Axial Turbine Stage Profile Cascades. *Sci. innov.*, 21(2), 73—87. https://doi.org/10.15407/scine21.02.073

Bladed rotary machines have existed and been actively utilized across various industries for over a century [1—7]. A significant portion of their applications has been concentrated in axial-type turbines and turboexpanders, including steam turbines [5], gas power turbines [6], aviation gas turbine engines (GTEs) [7, 8], transportation GTEs, and other systems [9]. Due to accumulated experience and continuous research, effective methods and approaches for designing axial turbines have been developed [10—15]. Based on these approaches, axial turbines of various types have been continuously designed, manufactured, and implemented [16, 17]. Leading companies in this field, such as *General Electric*, *Siemens*, *Pratt & Whitney*, *Mitsubishi*, *Rolls-Royce*, *Ukrenergomash* (*Turboatom*), and *Ivchenko-Progress*, have achieved significant success.

The design of a turbine is a complex multiparametric problem requiring consideration of numerous factors, including efficiency, lifespan, cost, mass and dimensional characteristics, and others [17]. One of the key aspects that receives significant attention in turbine design is gas-dynamic efficiency [18]. Ultimately, the gas-dynamic efficiency of turbines is determined by the irreversible losses of kinetic energy in the actual flow process compared to the ideal, usually isentropic, process [19].

Modern design methodologies and manufacturing technologies have enabled the creation of axial turbines with sufficiently high gas-dynamic efficiency [20—23]. It has become almost standard for new turbines to exhibit kinetic energy losses of less than 10% under nominal operating conditions, and in some cases, significantly lower [24—28]. Despite this progress, the pursuit of further gas-dynamic improvements in axial turbines has remained highly relevant and continues to be an active area of research [29—33]. This raises the critical question about the realistically achievable minimum kinetic energy loss in an axial turbine under given operating conditions.

Kinetic energy losses can be categorized as profile losses, trailing edge losses, tip leakage losses, secondary flow losses, wave losses, unsteady flow losses, separation and vortex losses, among others [25]. This classification remains somewhat conditional, as different types of losses are often interrelated, complicating the analysis of individual contributing factors [29]. This study presents research findings aimed at identifying the correlations between various influencing factors and losses, as well as estimating the practically attainable minimum kinetic energy loss in an axial turbine stage, without accounting for the spatial structure of the flow. The research has been conducted using advanced numerical methods for gas-dynamic calculations and turbine flow path design. To artificially eliminate the impact of three-dimensional flow effects, the study has considered simplified two-dimensional turbine stage geometries, replacing blades with profile cascades. To refine the research scope, turbine stages have been designed in accordance with long-standing global expertise and established turbomachinery design recommendations, including the experience of the authors [34—41].

The numerical investigation of three-dimensional steam flow and the design of the flow path of a steam turbine have been conducted using the IPMFlow software package, which has been developed as an extension of the FlowER and FlowER-U programs [37]. The mathematical model implemented in this package is based on the numerical integration of Reynolds-averaged unsteady Navier-Stokes equations using an implicit, quasi-monotonic ENO scheme of enhanced accuracy and the two-parameter differential SST turbulence model by Menter [39]. To account for the real thermodynamic properties of the working fluid, an interpolation-analytical method has been applied for approximating complex equations of state, using the IAPWS-95 formulation and modified Benedict-Webb-Rubin equations [34, 38]. Computational results obtained using the IPMFlow software package have demonstrated the necessary reliability in both the qualitative flow structure and the quantitative assessment of characteristics for isolated turbine cascades and the flow

paths of turbomachinery as a whole [36]. To accelerate computation time, an original parallel computing technology has been integrated into the IPMFlow package [41].

The spatial configuration of the blade row in an axial flow path has been developed using the analytical profiling method [37, 40, 41], in which the blade shape is defined by an arbitrary set of planar profiles described by fourth- and fifth-order curves. A limited set of parameterized values has been used as input data, most of which are widely accepted in turbine engineering, including profile width, number of blades, inlet flow angle, and effective outlet angle from the cascade. This method enables the rapid generation of complete spatial configurations for a wide range of axial turbine flow paths, making it a highly effective and convenient tool for solving gas-dynamic design and optimization problems in turbomachinery.

The study has focused on two of the most common axial turbine stage configurations — active and reactive types. These stages have been modeled using planar profile cascades to eliminate the influence of spatial effects on gas-dynamic characteristics, such as tip leakage losses, secondary flows, and blade row divergence. The dimensionless parameter u/c_{0t} (where u is the circumferential velocity of the rotor cascade, and c_{0t} is the conditional velocity of thermal drop across the stage) has been maintained at values of 0.5 and 0.7. The reactivity coefficient has been set to range within 0.1—0.2, for the active stages, and within 0.5—0.6, for the reactive stages, while ensuring that the exit flow direction remains close to axial. The study has examined the impact of the effective stator angle α_{1ef} (in absolute motion) and the dimensionless parameters Re_{ex} (Reynolds number at the stage outlet) and λ_{0t} (dimensionless conditional velocity of thermal drop across the stage) on the gas-dynamic characteristics of the turbine stages. To this end, the following considerations on the variables have been made:

- α_{1ef} is equal to 71°, 74°, 77° and 80° (measured from the axial direction);
- the circumferential velocity of the rotor cascade u, with five values taken for both active and reactive stages;
- Three options of P_{in}^{*} (the total pressure of the stagnated flow at the stage inlet);
- Three options of b_x (the axial width of the rotor cascade).

The total temperature of the stagnated flow at the inlet, T_0^{*} has been kept constant, while the static pressure at the outlet has been set to ensure the required u/c_{0t}. Using formulas (1)—(3), the values of the parameters under investigation have been computed to analyze their impact on stage characteristics.

$$c_{0t} = \sqrt{2(h_{in}^{*} - h_{iz\,ex})}, \tag{1}$$

$$\lambda_{0t} = \frac{c_{0t}}{a_{t0}} = \frac{c_{0t}}{\sqrt{\gamma R T_0^{*}}}, \tag{2}$$

$$Re_{ex} = \left(\frac{\rho C b_x}{\mu} \right)_{ex}. \tag{3}$$

where h_{in}^{*} is the enthalpy of the stagnated flow at the stage inlet, $h_{iz\,ex}$ is the isentropic enthalpy at the stage outlet, a_{0t} is the velocity based on the stage inlet parameters, γ is the adiabatic index for an isentropic process, R is the gas constant, ρ is the density, μ is the dynamic viscosity, and C is the absolute flow velocity.

For each computational point, a new stage design for the profile cascades has been developed. The stages have been created following the principle of "rational" design using proprietary methods described earlier. Gas-dynamic calculations have been performed on a structured grid with approximately 15,000 cells. The dimensionless parameter $y+$ near solid surfaces has not exceeded 5. To simplify the study, the authors have used the thermal equation of state for an ideal gas $P = R\rho T$ [42, 43], with superheated steam as the working media characterized by the constants R = 387 J/(kg · K) and γ = 1.3. The shape of the profile stage flow part, which under specific conditions exhibits gas-dynamic efficiency close to optimal, has been selected based on the principle

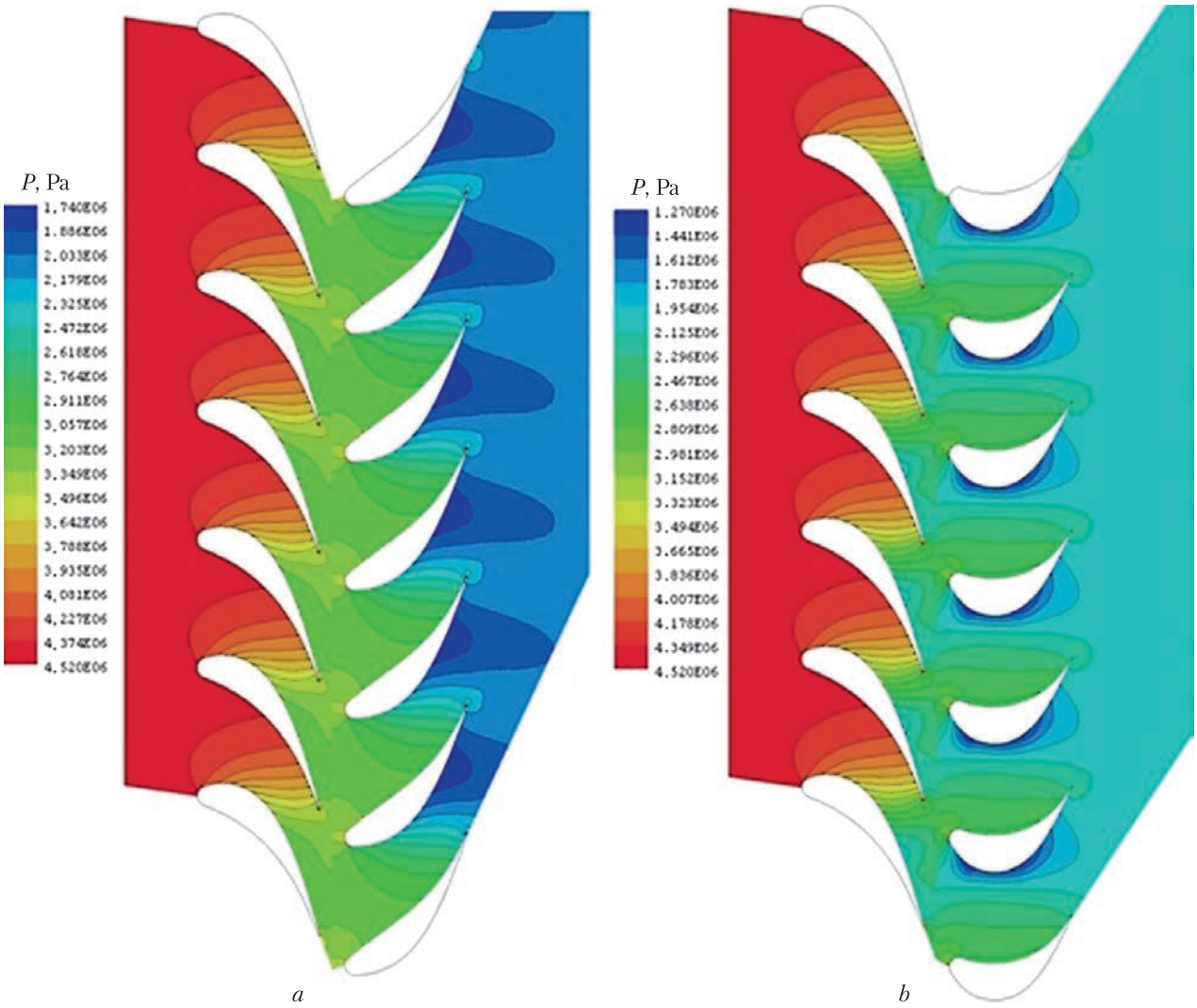

Fig. 1. Static pressure isolines at $\alpha_{1ef} = 71°$: *a* — reactive profile stage; *b* — active profile stage

of "rational" design. This approach does not rely on classical optimization methods [3, 5, 14] but is instead grounded in expert experience and variational calculations. Stage calculations have been conducted in a quasi-stationary formulation [44], where gas-dynamic parameters at the interface boundaries of the stator and rotor computational domains have been circumferentially averaged and subsequently applied as boundary conditions for the adjacent cascade.

Figures 1—2 provide an example visualization of static pressure isolines for four computational points of profile cascade stages at u/c_{0t} equal to 0.7 and 0.5 (reactive and active stages, respectively) and α_{1ef}, of 71° and 80°.

The presented static pressure distribution isolines are characteristic of reactive and active-type stages. In reactive stages, the flow exhibits a converging pattern in both the stator and rotor (Fig. 1, *a*, Fig. 2, *a*). Under these conditions, the flow accelerates while the static pressure decreases. In active-type stages (Fig. 1, *b*, Fig. 2, *b*), the flow remains converging only within the stator grid. In the rotor grid, the flow undergoes

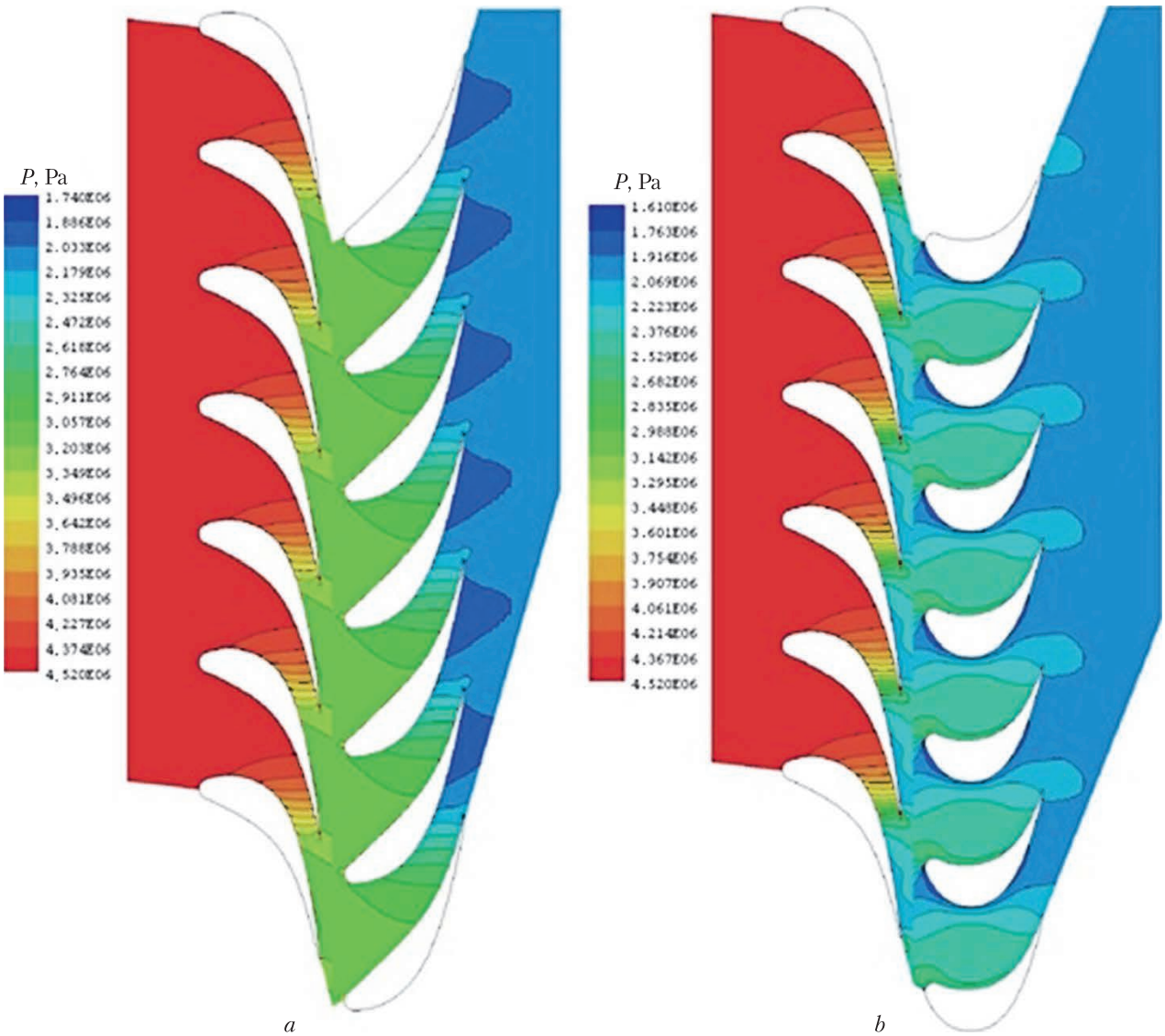

Fig. 2. Static pressure isolines at $\alpha_{1ef} = 80°$: *a* — reactive profile stage; *b* — active profile stage

minimal acceleration, and the reduction in static pressure is significantly smaller compared to the stator. Generally, under identical conditions, reactive profile stages have exhibited greater aerodynamic efficiency than active ones [7, 13].

Figure 3 shows the dependences kinetic energy losses ξ_{st} in the stages on c_{0t} at various α_{1ef} and u/c_{0t}. All the presented results have been calculated at identical values of P^*_{in}. The kinetic energy losses in the stage are determined by the following formula:

$$\xi_{st} = \frac{h_{ex} - h_{iz\,ex}}{h^*_{in} - h_{iz\,ex}} \cdot 100\%, \qquad (4)$$

where h_{ex} is the enthalpy at the stage outlet.

The presented results have indicated that for all configurations of active and reactive stages and values of α_{1ef}, the dependence patterns of kinetic energy losses ξ_{st} are similar. Within the con-

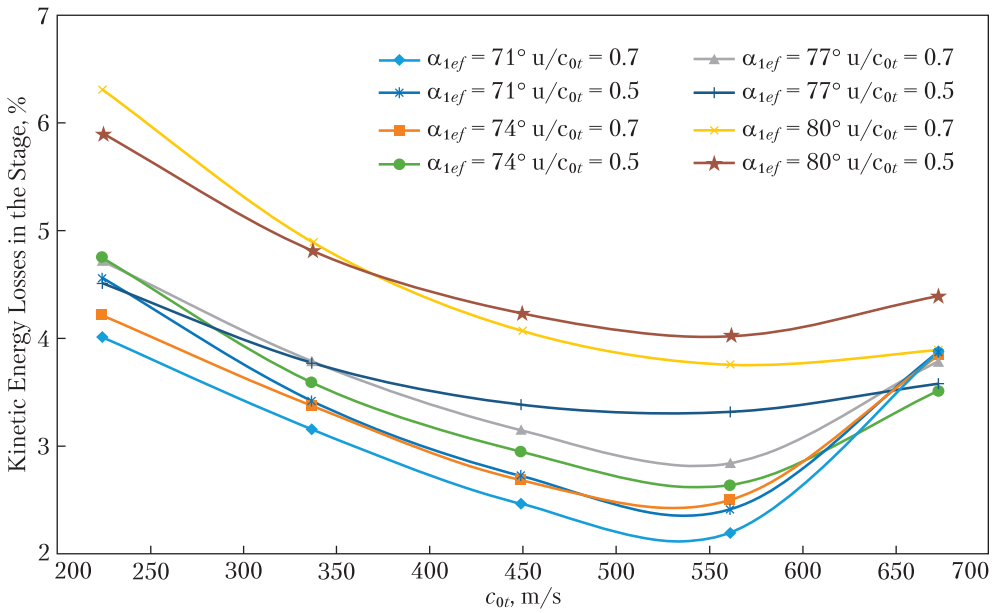

Fig. 3. Kinetic energy losses in a stage as a function of c_{0t}

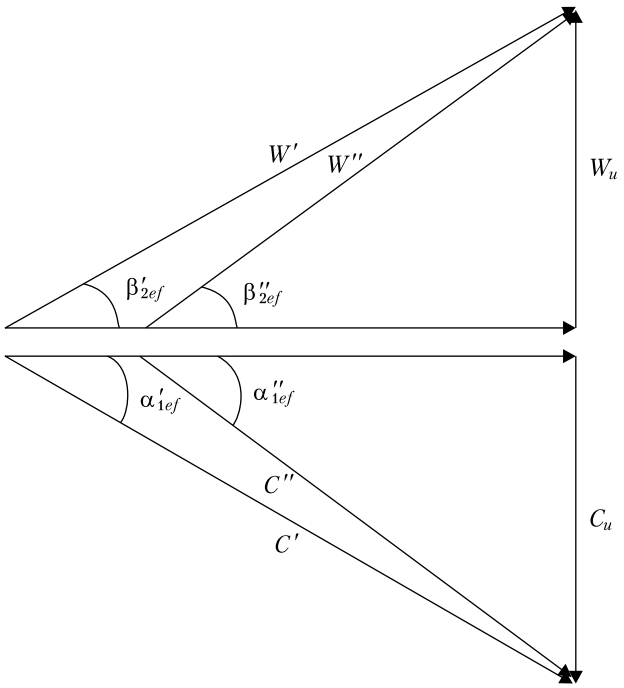

Fig. 4. Triangles of velocities

sidered ranges, these dependencies exhibit nearly smooth curves with a single minimum. For the dependencies on c_{0t} (Fig. 3), at identical α_{1ef}, the kinetic energy losses in the reactive stages are lower across almost the entire range as compared with the active stages. Additionally, for all stages, as α_{1ef} decreases, so do the kinetic energy losses. Among all the analyzed configurations, the lowest losses have been achieved for the reactive stage with the smallest $\alpha_{1ef} = 71°$.

As previously mentioned, under equal conditions, the higher efficiency of reactive stages has been well-documented [7, 13, 20] and is explained by a more uniform load distribution between the stator and the rotor, resulting in a convergent flow character in both components.

The reduction in the kinetic energy losses with decreasing α_{1ef}, in the authors' opinion, is attributed to two primary reasons. First, as α_{1ef} decreases, so does the angle β_{2ef} (the effective rotor angle in relative motion) in absolute value. This is clearly visible when comparing the rotor grid shapes between the configurations in Figs. 1, *a* and 2, *a* (reactive stages) and Fig. 1, *b* and 2, *b* (active stages). Thus, as the angles α_{1ef} and β_{2ef} decrease, and so do the flow turning angles, which reduces shear between the flow layers and, consequently, lowers kinetic energy losses.

ISSN 2409-9066. Sci. innov. 2025. 21(2)

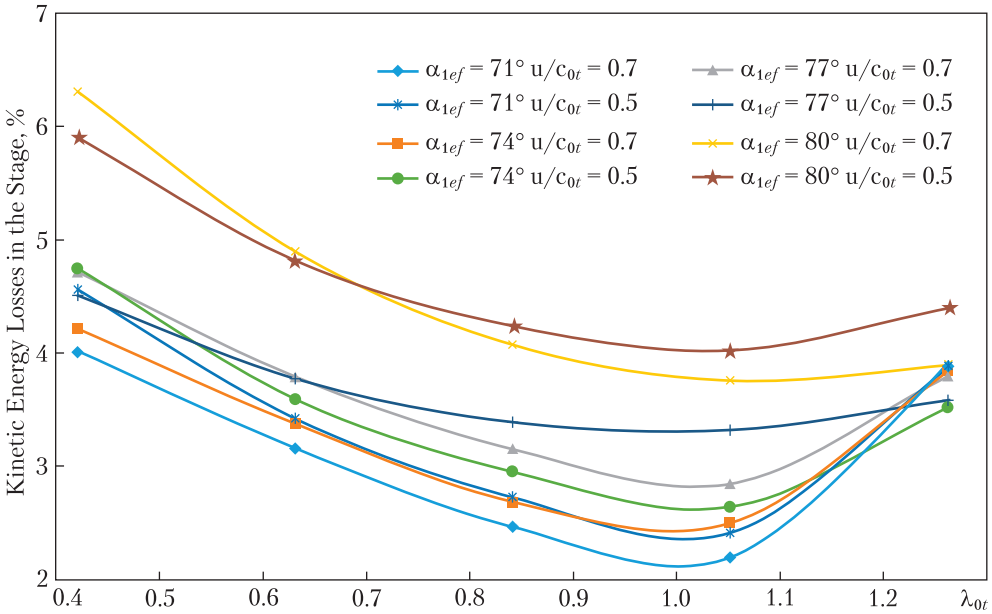

Fig. 5. Kinetic energy losses in stage as function of λ_{0t}

The second reason is related to the fact that, under other equal conditions, as the angles α_{1ef} and β_{2ef} decrease, the mean flow velocity in absolute motion within the stator C and in the moving coordinate system within the rotor W increases. This can be explained by the need to maintain approximately equal circumferential velocities in absolute motion within the stator C_{u1} and in the moving coordinate system within the rotor W_{u2}, regardless of α_{1ef} and β_{2ef}, to ensure the same thermal drop across the stage (the same c_{0t} values). The analysis of the velocity triangles (Fig. 4) has shown that at the constant circumferential velocities C_{u1} and W_{u2}, the total velocities C and W increase as α_{1ef} and β_{2ef} decrease, and vice versa. As C and W grow, the Reynolds numbers increase, which leads to a reduction in the thickness of the boundary layers and in the kinetic energy dissipation.

Figure 3 also demonstrates that in the initial part of all dependencies, an increase in c_{0t} leads to a decrease in kinetic energy losses. However, after reaching a minimum, the losses begin to increase. Notably, the position of this minimum remains approximately the same across all considered cases with respect to c_{0t}.

The reduction in kinetic energy losses with increasing c_{0t} can be attributed to the corresponding increase in flow velocities within the rotor and stator cascades. As previously mentioned, this results in higher Reynolds numbers, which contribute to a reduction in the boundary layer thickness and, consequently, to a lower energy dissipation.

The minimum in the kinetic energy losses at a certain value of c_{0t}, followed by an increase in ξ_{st}, as c_{0t} continues to grow, can be explained by analyzing the dependencies presented in Fig. 5. In this case, instead of examining the dependence on c_{0t}, the relationship is expressed in terms of the parameter λ_{0t}. As evident from Figs 3 and 5, the trends in both dependencies appear identical.

The minimum values of kinetic energy losses approximately coincide with $\lambda_{0t} = 1$. This indicates that at $\lambda_{0t} \geqslant 1$, the flow reaches supersonic velocities, which leads to the emergence of so-called "wave" losses [29, 42, 43]. This contributes to an overall increase in the kinetic energy losses. As λ_{0t} continues to increase, the wave losses become even more pronounced, further intensifying the kinetic energy losses in the flow.

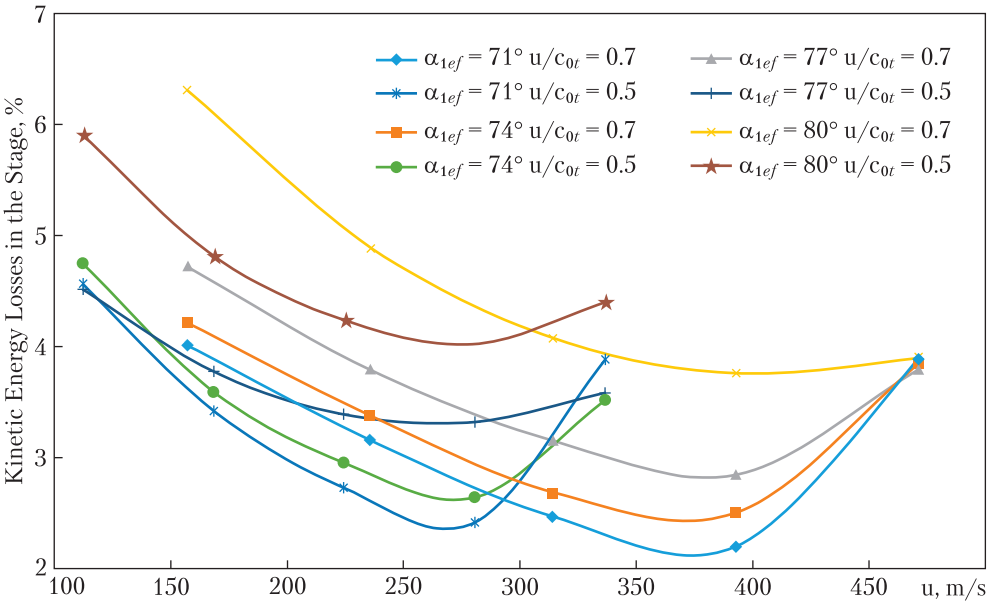

Fig. 6. Kinetic energy losses in the stage as function of u

As previously mentioned, within the analyzed ranges, for the reactive stage, the global minimum of kinetic energy losses has been achieved at $u/c_{0t} = 0{,}7$, $\alpha_{1ef} = 71°$, $\lambda_{0t} \approx 1$. Furthermore, having analyzed Fig. 3, we suggest that the thermal drop assigned to the stage (determined by c_{0t}) can be most efficiently utilized by the reactive stage (at $u/c_{0t} = 0{,}7$) To maintain $u/c_{0t} = 0{,}7$ at a given c_{0t}, it is necessary to ensure an appropriate rotor grid velocity u. However, it should be noted that achieving the required (high) values of u is often constrained due to various factors. Figure 6, similar to Figs. 3 and 5, presents the dependencies of kinetic energy losses ξ_{st} in the stages on u for various α_{1ef} and u/c_{0t}.

The presented results indicate that there is a velocity range for u (at lower values) in which active stages have proven to be more efficient. Furthermore, active stages allow for a greater thermal drop to be utilized at fixed values of u compared to reactive stages. This enables the design of multistage turbines with a reduced number of stages, which is advantageous in terms of mass, dimensional, and cost characteristics.

As previously mentioned, Reynolds numbers influence kinetic energy losses. Figure 7 illustrates the dependencies of kinetic energy losses on Reynolds numbers, based on the flow parameters at the stage outlet (Re_{ex}).

The dependencies for active and reactive stages with $\alpha_{1ef} = 71°$, which has demonstrated the highest efficiency, have been presented. To investigate a broader range of Reynolds number variations, in addition to the baseline total inlet pressure P^*_{in} (P_2), two additional pressure levels, P_1 and P_3, have been considered. Similarly, besides the baseline characteristic width of the rotor cascade b_{x2}, two additional sizes, b_{x1} and b_{x3}, have been analyzed. The relationships between these variations are as follows: $b_{x1} < b_{x2} < b_{x3}$ and $P_1 < P_2 < P_3$.

The presented results clearly indicate that for similar configurations with identical values of α_{1ef}, u/c_{0t} and c_{0t}, kinetic energy losses decrease as the Reynolds number Re_{ex} increases. Additionally, Fig. 7 shows two curves that pass through the minimum points of kinetic energy losses for reactive and active stages, respectively. It can be stated with high confidence that these curves coincide with the isolines of $\lambda_{0t} = 1$. Similarly, other isolines corresponding to different values of λ_{0t} can be identified.

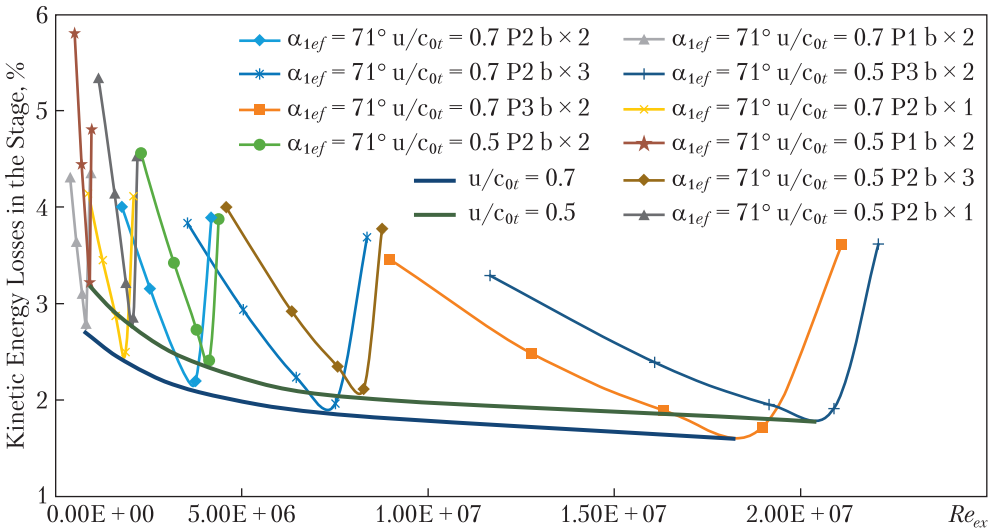

Fig. 7. Kinetic energy losses in the stage as function of Re_{ex}

Theoretically, the minimum kinetic energy losses should approach zero. However, achieving such a result in practice is impossible. Given that the profile stages for each considered operating point have been designed based on the "rational" design principle described earlier, the isolines of the curves at $\lambda_{0t} = 1$ represent the minimum achievable kinetic energy losses for the corresponding Reynolds numbers of reactive and active stages. The authors believe that these results have been obtained for the first time globally.

Similar to the isolines of $\lambda_{0t} = 1$, it is possible to construct isolines for other values of λ_{0t} та α_{1ef} in the context of kinetic energy loss dependencies. The diagrams obtained in this manner could serve as a comprehensive data set for designing profile cascade stages across a broad range of operating parameters for real flow parts in axial turbines.

Up to this point, the analysis has focused on the influence of operating parameters on kinetic energy losses in profile stages. Indeed, this is one of the primary characteristics determining the energy efficiency of a stage. For "internal" stages, meaning those followed directly by additional stages, efficiency considerations can be primarily based on this parameter. However, the situation differs when considering the final stages of a flow part — whether within a turbine cylinder or the entire turbine itself. In such cases, the overall efficiency of both the stage and the turbine is significantly affected by outlet velocity losses:

$$\xi_{ov} = \frac{c_{ex}^2 / 2}{h_{in}^* - h_{iz\,ex}} \cdot 100\%, \qquad (5)$$

where ξ_{ov} is the kinetic energy losses due to outlet velocity; C_{ex} represents the absolute velocity of the flow at the stage outlet.

Indeed, in the last stages, the kinetic energy of the exiting flow is lost, whereas in the internal stages, this energy is transferred to the subsequent stages. Therefore, for the last stages, it is necessary to reduce the outlet velocity of the flow, using total kinetic energy losses as the efficiency criterion:

$$\xi_{st}^* = \xi_{st} + \xi_{ov}, \qquad (6)$$

where ξ_{st}^* is the total kinetic energy losses.

Figures 8—10, similarly to Figs. 3, 5, and 6, show the total kinetic energy losses in various stages as function of c_{0t}, λ_{0t}, and u.

The presented results have indicated that, unlike the losses calculated without considering outlet velocity losses, the gas-dynamic efficiency is higher in stages with a greater α_{1ef}. Among the

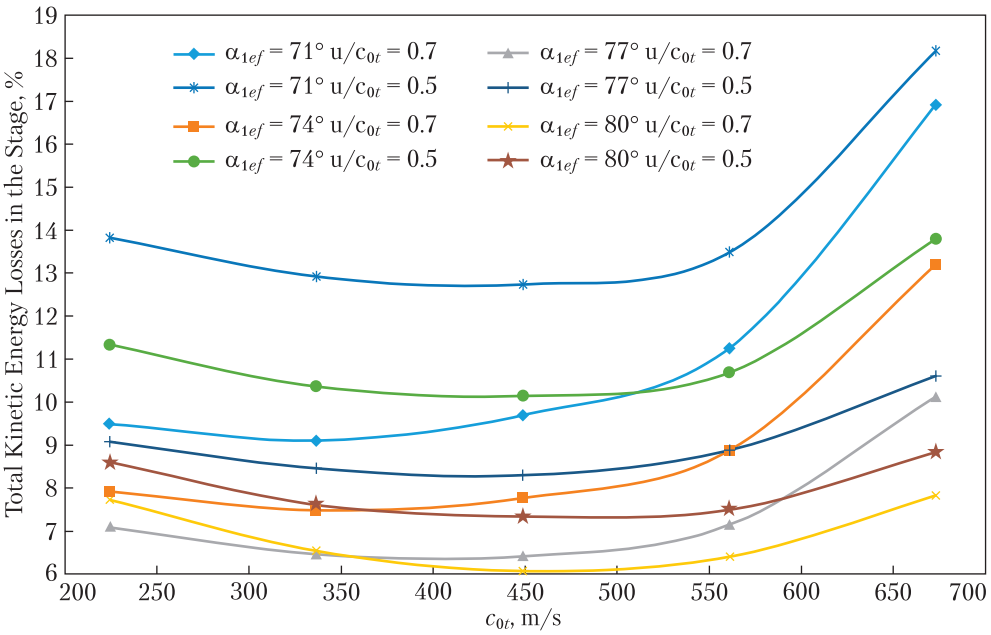

Fig. 8. Total kinetic energy losses in a stage as function of c_{0t}

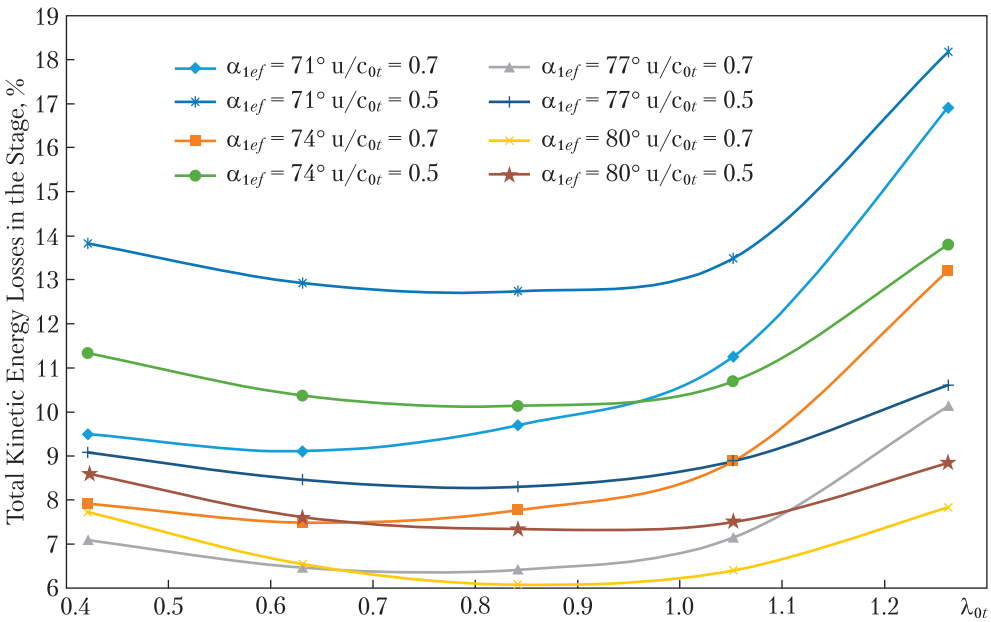

Fig. 9. Total kinetic energy losses in a stage as function of λ_{0t}

studied cases, the highest gas-dynamic efficiency is achieved in the reactive stage at $\alpha_{1ef} = 80°$. This finding suggests that the design approaches for internal and last stages should differ.

Using validated numerical methods for gas-dynamic analysis and design of the flow parts in bladed turbomachinery, a comprehensive study has been conducted on the influence of opera-

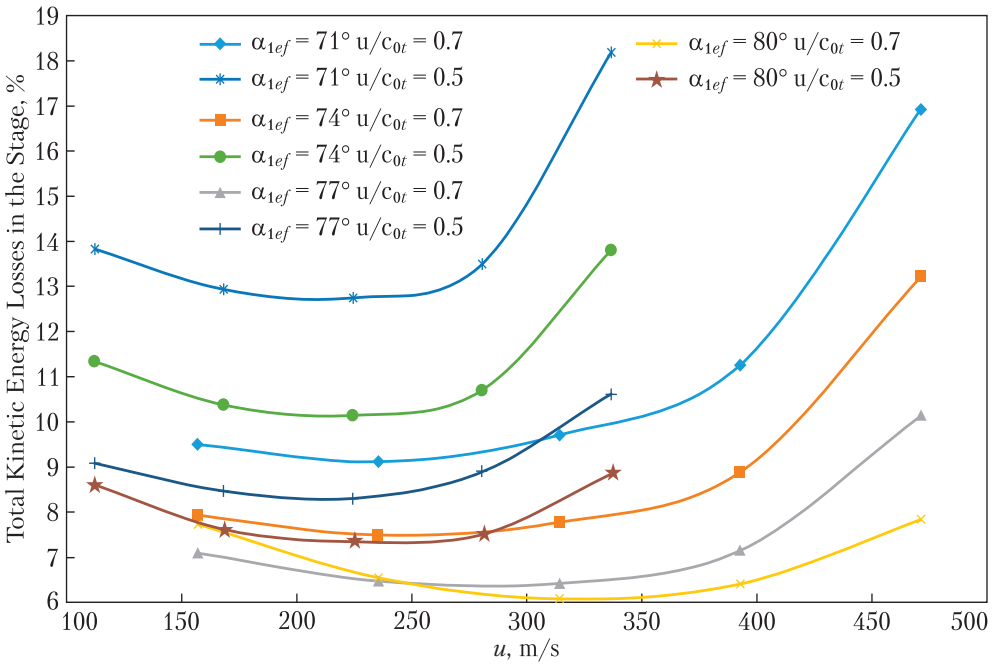

Fig. 10. Total kinetic energy losses in a stage as function of u

tional and geometric characteristics on the efficiency of blade row stages in axial turbines.

For each of the analyzed operating points, defined by specific operational and geometric parameters, blade row stages have been designed based on the principle of "rational" design, ensuring that their gas-dynamic efficiency is close to the theoretical maximum.

As a result of this study, the following new findings and patterns have been identified:

1. The kinetic energy losses in the stages reach their minimum for all cases at $\lambda_{0t} \approx 1$. These losses decrease as λ_{0t} increases from 0 to 1 due to the increase in flow velocity and, consequently, the Reynolds number. However, when λ_{0t} exceeds 1, kinetic energy losses begin to rise due to wave-induced losses (flow wave crisis).

2. In general, the reactive blade rows ($u/c_{0t} = 0.7$) tend to achieve lower kinetic energy losses as compared with the active blade rows ($u/c_{0t} = 0.5$). However, in many cases, due to the inability to meet the required operating conditions — particularly the high circumferential velocity u (exceeding 290—310 m/s) — active blade rows ($u/c_{0t} = 0.5$) may exhibit lower kinetic energy losses.

3. A decrease in α_{1ef} leads to a reduction in kinetic energy losses in both active and reactive stages (for both values of u/c_{0t}). This effect is attributed to the reduced flow turning angle within the turning blade rows.

4. For the first time, dependencies of the minimum achievable kinetic energy losses for the corresponding Reynolds numbers of the reactive and active blade rows in axial stages have been obtained. As the Reynolds number increases, these losses in the stages decrease. At $Re \geqslant 10^7$, a region with properties close to self-similarity begins.

5. The kinetic energy losses associated with the exit velocity are lower for the reactive stages ($u/c_{0t} = 0.7$). They decrease as α_{1ef} increases and the theoretical thermal drop c_{0t} goes down.

6. The operating and other stage characteristics (u/c_{0t}, c_{0t}, α_{1ef}, etc.) affect the kinetic energy losses and outlet velocity losses in a different way. Therefore, the minimum (or near-minimum) total losses in the blade row stages are achieved when

there is maintained an optimal (rational) balance between the kinetic energy losses and the outlet velocity losses.

7. The last blade row stages should be designed to minimize the total kinetic energy losses, whereas the internal stages should focus solely on minimizing the kinetic energy losses.

8. When designing real (three-dimensional) stages, it is necessary to account for additional types of losses, such as the end losses (caused by secondary flows), the losses due to flow non-uniformity, and others.

The further research aims to develop diagrams representing the dependencies of kinetic energy losses in blade row stages on α_{1ef}, Re_{ex} і λ_{0t}. These diagrams will serve as a foundational dataset (a first approximation) for designing blade row stages across a wide range of operating conditions in real axial turbine flow parts.

This research was conducted with the support of the program *R&D in the Priority Area of Heat, Electric, and Nuclear Energy Technologies for Ensuring Ukraine's Energy Security* for 2023—2024.

REFERENCES

1. Bloch, H. P., Murari, P. S. (2009). *Steam Turbines: Design, Applications, and Rerating*. New York.
2. Shao, S., Deng, Q. H., Feng, Z. P. (2013, June). Aerodynamic optimization of the radial inflow turbine for a 100kW-class micro gas turbine based on metamodel-semi-assisted method. *In Proceedings of the ASME Turbo Expo 2013* (3—7 June 2013, San Antonio). San Antonio. https://doi.org/10.1115/GT2013-95245
3. Guo, Z. D., Song, L. M., Zhou, Z. M., Li, J., Feng, Z. P. (2015). Aerodynamic analysis and multi-objective optimization design of a high pressure ratio centrifugal impeller. *J. Eng. Gas Turbines Power*, 092602—14. https://doi.org/10.1115/GT2014-25496
4. Witanowski, L., Klonowicz, P., Lampart, P., Klimaszewski, P., Suchocki, T., Jedrzejewski, L., Zaniewski, D., Ziółkowski, P. (2023). Impact of rotor geometry optimization on the off-design ORC turbine performance. *Energy*, 265, art. no. 126312 https://doi.org/10.1016/j.energy.2022.126312.
5. Wu, R., Liu, D., Zheng, J., Tong, J., Ye, X. (2024). Optimization on Main Steam Pressure of a Steam Turbine Under Low Loads Based on IGWO-SVM. *Dongli Gongcheng Xuebao/Journal of Chinese Society of Power Engineering*, 44 (7), 1042—1050. https://doi.org/10.19805/j.cnki.jcspe.2024.230345.
6. Miyoshi, I., Higuchi, S., Kishibe, T. (2013). Improving the performance of a high pressure gas turbine stage using a profiled endwall. *Proceedings of the ASME Turbo Expo*, 6 A. https://doi.org/10.1115/GT2013-95148
7. Zhang, R., Zhang, W., Gan, M., Xiao, W., Zeng, F., Zhao, D. (2024). Toward high-lift low-solidity design for incidence tolerant gas turbine blade profile. *Energy*, 309, art. no. 133034. https://doi.org/10.1016/j.energy.2024.133034
8. Zou, Z., Wang, S., Liu, H., Zhang, W. (2018). Axial turbine aerodynamics for aero-engines: Flow analysis and aerodynamics design. *Axial Turbine Aerodynamics for Aero-Engines: Flow Analysis and Aerodynamics Design*, 1—563. https://doi.org/10.1007/978-981-10-5750-2
9. Guzović, Z., Kastrapeli, S., Budanko, M., Klun, M., Rašković, P. (2024). Improving the thermodynamic efficiency and turboexpander design in bottoming organic Rankine cycles: The impact of working fluid selection. *Energy*, 307, art. no. 132642. https://doi.org/10.1016/j.energy.2024.132642.
10. Abdalhamid, A.M.K., Eltaweel, A. (2024). Design and analysis of a single-stage supersonic turbine with partial admission. *Energy*, 309, art. no. 133100. https://doi.org/10.1016/j.energy.2024.133100
11. Denton, J. D. (2017, June). Multall: An Open Source, CFD Based, Turbomachinery Design System. *Proceedings of the ASME Turbo Expo 2017: Turbomachinery Technical Conference and Exposition. Volume 2B: Turbomachinery (June 26—30, 2017, Charlotte, North Carolina, USA)*. Charlotte, North Carolina.
12. Zhang, M., He, L. (2015). Combining shaping and flow control for aerodynamic optimization. *AIAA Journal*, 53(4), 888—901. https://doi.org/10.2514/1.J053277
13. Wilson, D., Korakianitis, T. (2014). *The Design of High-Efficiency Turbomachinery and Gas Turbines*. Cambridge, MA.
14. Arko, B. M., McQuilling, M. (2013). Computational study of high-lift low-pressure turbine cascade aerodynamics at low Reynolds number. *Journal of Propulsion and Power*, 29(2), 446—459. https://doi.org/10.2514/1.B34576
15. Michalek, J., Straka, P. (2013). A comparison of experimental and numerical studies performed on a low-pressure turbine blade cascade at high-speed conditions, low Reynolds numbers and various turbulence intensities. *Journal of Thermal Science*, 22(5), 413—423. https://doi.org/10.1007/s11630-013-0643-9

16. Ghelani, R., Roumeliotis, I., Saias, C. A., Mourouzidis, C., Pachidis, V., Norman, J., Bacic, M. (2024). Integrated Hybrid Engine Cycle Design and Power Management Optimization. *Journal of Engineering for Gas Turbines and Power*, 146(10), art. no. 101007. https://doi.org/10.1115/1.4065020
17. Badum, L., Schirrecker, F., Cukurel, B. (2024). Multidisciplinary Design Methodology for Micro-Gas-Turbines — Part I: Reduced Order Component Design and Modeling. *Journal of Engineering for Gas Turbines and Power*, 146(10), art. no. 101001. https://doi.org/10.1115/1.4064825
18. Du, Z., Cai, L., Zeng, J., Chen, Y., Zhou, X., Wang, S. (2024). Enhancing Aerodynamic Performance of a Non-Axisymmetric Endwall Contoured Cascade Through Section Profiling Method. *Journal of Turbomachinery*, 146(12), art. no. 121004. https://doi.org/10.1115/1.4065859
19. Duan, P. H., He, L. (2024). Design Optimization of Blade Tip in Subsonic and Transonic Turbine Stages — Part I: Stage Design and Preliminary Tip Optimization. *Journal of Engineering for Gas Turbines and Power*, 146(9), art. no. 091001. https://doi.org/10.1115/1.4064325
20. Giel, P. W., Shyam, V., Juangphanich, P., Clark, J. P. (2020). Effects of trailing edge thickness and blade loading distribution on the aerodynamic performance of simulated CMC turbine blades. *Proceedings of the ASME Turbo Expo*, 2B-2020, art. no. V02BT33A028. https://doi.org/10.1115/GT2020-15802
21. Wang, K., Chen, F., Yu, J., Song, Y., Ghorbaniasl, G. (2023). Effect of uncertain operating conditions on the aerodynamic performance of high-pressure axial turbomachinery blades. *Energy*, 283, art. no. 128991. https://doi.org/10.1016/j.energy.2023.128991
22. Wang, X., Li, W., Zhu, Y., Zuo, Z., Chen, H. (2021). Optimal design and flow loss reduction mechanism of bowed guide vane in a compresses-air energy storage axial flow turbine. *Energy Stor. Sci. Tech.*, 10(5), 1524—1535. https://doi.org/10.19799/j.cnki.2095-4239.2021.0338
23. Ghandi, H., Togh, R. A., Tousi, A. M. (2020). Investigation on the aerodynamic performance and boundary layer characteristics of high deflection industrial turbine cascade at off-design conditions. *Journal of Mechanical Science and Technology*, 34(12), 5261—5269. https://doi.org/10.1007/s12206-017-1247-1
24. Li, L., Zhang, W., Li, Y., Zhang, R., Liu, Z., Wang, Y., Mu, Y. (2024). A non-parametric high-resolution prediction method for turbine blade profile loss based on deep learning. *Energy*, 288, art. no. 129719. https://doi.org/10.1016/j.energy.2023.129719
25. Duan, P., Tan, C. S., Scribner, A., Malandra, A. (2018). Loss generation in transonic turbine blading. *Journal of Turbomachinery*, 140(4), art. no. 041006. https://doi.org/10.1115/1.4038689
26. Miki, K., Ameri, A. (2024). Numerical Investigation of the Effect of Trailing Edge Thickness of Simulated Ceramic Matrix Composite Blades on Loss Profiles. *Journal of Turbomachinery*, 146(9), art. no. 091009. https://doi.org/10.1115/1.4065184
27. Miki, K., Ameri, A. (2022). Improved Prediction of Losses With Large Eddy Simulation in a Low-Pressure Turbine. *Journal of Turbomachinery*, 144(7), art. no. 071002. https://doi.org/10.1115/1.4053234
28. Przytarski, P. J., Wheeler, A. P. S. (2021). Accurate prediction of loss using high fidelity methods. *Journal of Turbomachinery,* 143(3), 1—13. https://doi.org/10.1115/GT201877125.
29. Vazquez, R., Antoranz, A., Cadrecha, D., Armananzas, L. (January, 2016). The Influence of Reynolds Number, Mach Number and Incidence Effects on Loss Production in Low Pressure Turbine Airfoils. *ASME Turbo Expo*. Paper No. GT2006-91121 https://doi.org/10.1115/GT2006-91121
30. Dellacasagrande, M., Lengani, D., Simoni, D., Ubaldi, M., Granata, A. A., Giovannini, M., Rubechini, F., Bertini, F. (2023). Analysis of unsteady loss sensitivity to incidence angle variation in low pressure turbine. *Proceedings of the ASME Turbo Expo*, 13B, art. no. v13bt30a037. https://doi.org/10.1115/GT2023-103770
31. Wang, J., Yin, Z., Zhang, H., Tang, H., Xu, Y., Chen, H. (2023). Adaptive prediction of turbine profile loss and multi-objective optimization in a wide incidence range. *Proceedings of the Institution of Mechanical Engineers, Part C: Journal of Mechanical Engineering Science*, 237(12), 2696—2713. https://doi.org/10.1177/09544062221140969
32. Ohiemi, I. E., Sunsheng, Y., Singh, P., Li, Y., Osman, F. (2023). Evaluation of energy loss in a low-head axial flow turbine under different blade numbers using entropy production method. *Energy*, 274, art. no. 127262, https://doi.org/10.1016/j.energy.2023.127262
33. Guan, Y., Li, W., Zhu, Y., Wang, X., Zhang, Y., Chen, H. (2024). Energy loss analysis in two-stage turbine of compressed air energy storage system: Effect of varying partial admission ratio and inlet pressure. *Energy*, 305, art. no. 132214. https://doi.org/10.1016/j.energy.2024.132214
34. Rusanow, A. V., Lampart, P., Pashchenko, N. V., Rusanov, R. A. (2016). Modelling 3D steam turbine flow using thermodynamic properties of steam IAPWS-95. *Polish Maritime Research*, 23(1), 61—67. https://doi.org/10.1515/pomr-2016-0009

35. Yershov, S., Rusanov, A., Gardzilewicz, A., Lampart, P. (1999). Calculation of 3D viscous compressible turbomachinery flows. *American Society of Mechanical Engineers, Pressure Vessels and Piping Division (Publication)*, 397 II, 143—154.
36. Lampart, P., Yershov, S., Rusanov, A., Szymaniak, M. (2004). Tip leakage/main flow interactions in multi-stage HP turbines with short-height blading. *Proceedings of the ASME Turbo Expo 2004*, 5B, 1359—1367. https://doi.org/10.1115/GT2004-53882
37. Yershov, S., Rusanov, A., Shapochka, A., Lampart, P., Wirydczuk, J., Gardzilewicz, A. (2002). Shape optimization of two turbine stages using the deformed polyhedron method and a three-dimensional RANS solver. *Proceedings of the Institution of Mechanical Engineers, Part A: Journal of Power and Energy*, 216(2), 203—213. https://doi.org/10.1243/09576500260049214
38. Rusanov, A., Rusanov, R., Klonowicz, P., Lampart, P., Żywica, G., Borsukiewicz, A. (2021). Development and experimental validation of real fluid models for CFD calculation of ORC and steam turbine flows. *Materials*, 14(22), 6879. https://doi.org/10.3390/ma14226879
39. Rusanov, A., Rusanov, R. (2021). The influence of stator-rotor interspace overlap of meridional contours on the efficiency of high-pressure steam turbine stages. *Archives of Thermodynamics*, 42(1), 97—114. https://doi.org/10.24425/ather.2021.136949
40. Rusanov, A., Subotin, V., Shvetsov, V., Rusanov, R., Palkov, I., Chugay, M. (2022). Application of innovative solutions to improve the efficiency of the LPC flow part of the 220 MW NPP steam turbine. *Archives of Thermodynamics*, 43(1), 63—87. https://doi.org/10.24425/ather.2022.140925
41. Rusanov, A., Chugay, M., Rusanov, R. (2023). Advanced Computer Technologies in the New Flow Part Development for Reactive Type HPC Steam Turbine of T-100 Series. *Lecture Notes in Mechanical Engineering*, 55—63. https://doi.org/10.1007/978-3-031-18487-1_6
42. Liepman, H. W., Roshko, A. (2002). *Elements of gasdynamics*. Mineola, New York. 464 p.
43. Powers, J. M. (2019). *Lecture notes on gas dynamics*. Notre Dame, Indiana.
44. Liu, P. (2021). *A General Theory of Fluid Mechanics*. Springer Singapore. 649 p. https://doi.org/10.1007/978-981-33-6660-2

Received 27.01.2025
Revised 17.02.2025
Accepted 18.02.2025

Р.А. Русанов (https://orcid.org/0000-0003-2930-2574),
А.В. Русанов (https://orcid.org/0000-0002-9957-8974),
М.О. Чугай (https://orcid.org/0000-0002-0696-4527)

Інститут енергетичних машин і систем ім. А.М. Підгорного
Національної академії наук України,
вул. Комунальників, 2/10, Харків, 61046, Україна,
+380 57 293 0144, ipmach@ipmach.kharkov.ua

АНАЛІЗ ВПЛИВУ РЕЖИМНИХ І ГЕОМЕТРИЧНИХ ХАРАКТЕРИСТИК НА ЕФЕКТИВНІСТЬ РЕШІТОК ПРОФІЛІВ СТУПЕНІВ ОСЬОВИХ ТУРБІН

Вступ. Лопаткові роторні машини існують й активно використовуються у різних галузях понад сто років, зокрема й у турбінах і турбодетандерах осьового типу: парові та газові енергетичні турбіни, авіаційні газотурбінні двигуни тощо.

Проблематика. Сучасні методи проєктування і технології виробництва дозволяють створювати осьові турбіни з достатньо високою газодинамічною ефективністю, яка визначається незворотними втратами кінетичної енергії потоку в реальному процесі порівняно з ідеальним процесом, зазвичай, ізоентропним. На сьогодні стало майже нормою те, що в нових турбінах на номінальних режимах роботи втрати кінетичної енергії нижчі за 10 %. Актуальним є встановлення величини реального, мінімального значення втрат кінетичної енергії, якого можна досягти в осьовій турбіні для відповідних умов роботи.

Мета. Дослідження впливу режимних і геометричних характеристик — ефективний кут статора, числа Рейнольдса й безрозмірної умовної швидкості теплового перепаду на ступені, на ефективність активних і реактивних ступенів решіток профілів осьових турбін.

Матеріали й методи. Застосовано сучасні чисельні методи розрахунку й проєктування проточних частин турбомашин, реалізованих у вигляді програмного комплексу *IPMFlow*.

Результати. Отримано низку нових результатів і закономірностей підвищення газодинамічної ефективності ступенів решіток профілів осьових турбін. Для кожної з розглянутих точок із заданими режимними і геометричними параметрами розроблено за принципом «раціонального» проєктування ступені решіток профілів, газодинамічна ефективність яких близька до максимально можливої. Показано, що при числах Рейнольдса більших за 5×10^6, значення втрат кінетичної енергії у ступенях решіток профілів можуть бути нижчими 2 %.

Висновки. За результатами досліджень отримано низку нових результатів і закономірностей, які можуть бути застосовані при проєктуванні й модернізації осьових турбін з метою підвищення їхньої ефективності.

Ключові слова: методи проєктування, газодинамічна ефективність, проточна частина турбіни, активний ступінь, реактивний ступінь.